

The impact of carbon additives on lithium ion diffusion kinetic of LiFePO₄/C composites

Thanh Dinh Duc¹, Anh My-Thi Nguyen¹, Tru Nhi Nguyen¹, Hang Thi La^{2,3}, Phung My-Loan Le^{4,*}

ABSTRACT

Introduction: LiFePO₄/C composites were synthesized via physical mixing assisted solvothermal process. Different kinds of carbon materials were investigated including 0D (carbon Ketjen black), 1D (carbon nanotubes) and 2D (graphene) materials. X-rays diffraction patterns of carbon coated LiFePO₄ synthesized by solvothermal was indexed to pure crystalline phase without the emergence of second phase. LiFePO₄ platelets and rods were in range size of 80-200 nm and dispersed well in carbon matrix. The lithium ion diffusion kinetics was evaluated through the calculated diffusion coefficients to explore the impact of carbon mixing. **Methods:** In this work, we studied the structure, morphologies and the lithium ion diffusion kinetic of LiFePO₄/C composites for Li-ion batteries. Different characterization methods were used including powder X-rays (for crystalline structure); Transmission Electron Microscopy (for particle and morphologies observation) and Cyclic voltammetry (for electrochemical kinetic study). **Results:** The study indicated LiFePO₄/C composites were successfully obtained by mixing process and the electrochemical performance throughout the calculated diffusion coefficient was significantly improved by adding the carbon types. **Conclusion:** The excellent ion diffusion was obtained for composites LiFePO₄/Ketjen black (KB) and LiFePO₄/CNT compared to LiFePO₄/Graphene. KB could be a potential candidate for large-scale production due to low-cost, stable and high electrochemical performance.

Key words: Carbon materials, Composite, LiFePO₄, Lithium ion batteries, Lithium ion kinetics

¹University of Technology, Vietnam National University-Ho Chi Minh City, 268 Ly Thuong Kiet street, Ward 14, District 10, Ho Chi Minh City, Viet Nam

²Graduate University of Science & Technology – VAST, Viet Nam

³Vinh Long University of Technology Education (VLUTE), Viet Nam

⁴University of Science, Vietnam National University- Ho Chi Minh City, 227 Nguyen Van Cu street, Ward 4, District 5, Ho Chi Minh City, Viet Nam

Correspondence

Phung My-Loan Le, University of Science, Vietnam National University-Ho Chi Minh City, 227 Nguyen Van Cu street, Ward 4, District 5, Ho Chi Minh City, Viet Nam

Email: lmpfung@hcmus.edu.vn

History

- Received: 14-09-2018
- Accepted: 19-03-2019
- Published: 31-03-2019

DOI :

<https://doi.org/10.32508/stdj.v22i1.462>



Copyright

© VNU-HCM Press. This is an open-access article distributed under the terms of the Creative Commons Attribution 4.0 International license.



INTRODUCTION

With the rapid growth of technology, Li-ion batteries (LIBs) have gradually become one of the most innovative and potential energy storage devices for a variety of energy applications. Regarding this, materials development plays a crucial role to provide LIBs outstanding characteristics compared to conventional batteries¹⁻³. Following LiCoO₂, LiMn₂O₄ as cathode materials, olivine LiFePO₄ (LFP) has been considered the most compatible candidate for portable devices or larger scale energy storage nowadays. This material possesses various desired properties, such as a long flat plateau of 3.45 V over a large lithium solid solution, straightforward fabrication, environmental benignity, and safety in handling and operation⁴. Unfortunately, there remain two major obstacles including low lithium-ion diffusion coefficient (10⁻¹⁴-10⁻¹⁶ cm².s⁻¹) and poor electronic conductivity (< 10⁻⁹ S.cm⁻¹) which struggle the electrochemical performance and the commercialization of LFP^{5,6}.

A variety of solutions have been proposed to overcome these problems. There most effective strategies consist of nano-sizing grains, conductive carbon utilization, controlled off-stoichiometry, and

transition metals doping⁷⁻⁹. By using nanoscale LFP particles, the diffusion pathway of lithium ions into octahedral vacancies of LFP crystalline becomes shorter, and then the electrochemical performance could be enhanced. Till now, top-down (solid-state reactions) and bottom-up (co-precipitation, hydro/solvothermal, sol-gel) methods are two main routes to synthesize nanoscale LFP and its composites. Unlike the former, the bottom-up or solution-based methods are much interested due to energy-saving and due to the ease control of size and morphology. Meanwhile, in the second strategy, carbon materials play the role of forming a conductive network linking the LFP particles to improve its electron transport¹⁰. Additionally, carbon deposition or coating on the surface of LFP particles in a reducing atmosphere also helps to limit the growth or agglomeration of LFP particles¹¹. Since the outstanding revolution of carbon materials, the unique characteristics come up with their own shapes such as spheres¹²⁻¹⁵, nanotubes¹⁶⁻¹⁸, nanofibers^{19,20}, or sheets (graphene)²¹⁻²³. These advantages could be potentially exploited for different purposes of materials improvement. However, the morphology of carbon, if not properly integrated, sometimes restrains

Cite this article : Dinh Duc T, My-Thi Nguyen A, Nhi Nguyen T, Thi La H, My-Loan Le P. **The impact of carbon additives on lithium ion diffusion kinetic of LiFePO₄/C composites.** *Sci. Tech. Dev. J.*; 22(1):173-179.

lithium ion movements in olivine structure and decreases the energy density in LFP/C composite. Apart from the above approaches, multivalent cations are usually used as suitable dopants for LFP to enhance high current rate performance as well as reduce polarization¹⁴. However, this increase of conductivity is doubted whether dopants could penetrate easily into LFP lattice and conduct the formation of surface conductive phases⁸.

With an aim to increase the ionic conductivity of LFP, LFP/C composites with different carbon matrix including Ketjen black (KB), CNT and graphene (Gr) were prepared. By using the solvothermal technique, LFP particles are the nanoscale size, and hence the lithium ion diffusion pathway could be expectedly shortening. To evaluate the impact of carbon coating, Cyclic Voltammetry method was used to understand the electrochemical kinetic and calculate the lithium ion diffusion coefficient as well.

METHODS

Synthesis process

Carbon-coated LFP particles were prepared via solvothermal route. All the reagents are analytical grade and readily used without further purification. Precursors are lithium hydroxide monohydrate LiOH.H₂O (Fisher, USA), ferrous sulfate heptahydrate FeSO₄.7H₂O (Fisher, USA), phosphoric acid H₃PO₄ 85 wt.% (Fisher, USA). Carbon sources are Ketjen black EC-600JD (Azko Nobel, Dutch), multi-walled carbon nanotubes (Sigma-Aldrich, USA) and graphene (Fisher, USA). 10 wt.% of different kind of carbons was well-dispersed by ultrasonication in 10 mL ethanol for 1 h. After that, 1.2 g of LiOH.H₂O was dissolved in 50 mL of ethylene glycol (EG, 98.5%, Merck, Germany) and distilled water until the mixture was homogeneous. Subsequently, carbon was added and magnetically stirred for 10 min to obtain mixture 1. Likewise, mixture 2 was prepared by dissolving 2.7 g FeSO₄.7H₂O with 1 mL H₃PO₄ (99 %, Merck, Germany) in 50 mL EG/H₂O solvent under the inert atmosphere. Mixture 1 was slowly added to mixture 2, continuously magnetically stirred for several minutes and transferred into a Teflon-lined stainless-steel autoclave. The solvothermal reaction occurred at 180°C for 5 h. The obtained mixture was cooled down in ambient condition followed by filtration and drying. Finally, LFP/C powder was annealed in the tube furnace at 650°C for 3 h to obtain the composite.

Materials characterization

The synthesized materials were characterized by various advanced techniques. Powder X-ray diffraction (XRD) data was collected on Bruker D8 Advance (France) with Cu-K α 1 radiation ($\lambda = 1.54056 \text{ \AA}$) at 2θ range of 15° to 60°. Transmission electron microscopy (TEM) for particle size study and morphology evaluation were performed using JEOL JEM 1400 microscope (120 kV).

Electrochemical measurements

For electrochemical characterization, the prepared composites were laminated to thin film cathode for half-cell testing. LFP/C composite was grounded using mortar for approximately 2 h to obtain fine particles. Then, 5 wt.% poly(vinylidene fluoride-co-hexafluoropro-pylene) (PVdF-HFP) as a binder in the solution of N-methyl-pyrrolidone (NMP) was added to LFP/C composite and mixed until a homogeneous slurry was obtained. Then, the slurry was coated on an Al foil and dried in a vacuum chamber at 80°C for 14 h. The cathode foil was punched into 10 mm-diameter discs and used as working electrodes. Lithium metal foil was used as the anode while commercial Whatman glass-fiber membrane and the 1 M solution of LiPF₆ in EC: DMC (1:1) were used as separators and electrolyte, respectively. Finally, Swagelok cells were assembled in an argon-filled glove box. Cyclic voltammetry tests were performed on Bio-Logic MPG-2 battery tester (France) in the voltage range of 3.0-4.0 V (vs. Li⁺/Li) at room temperature. For each of composite material, the measurement was performed in three times repeated in two different cells.

RESULTS

Structural analysis

Crystalline structure and chemical composition of LiFePO₄ were evaluated, as shown in **Figure 1**. Comparing to XRD reference patterns, olivine LFP phase was successfully prepared with the index of Pnmb space group in orthorhombic system (ICDD no. 40-1499) without emerged impurities. Additionally, from **Figure 1**, typical diffraction peaks of LFP at $2\theta = 20.8^\circ$, 25.5° , 29.7° , 32.2° and 35.5° are sharp and relatively narrow indicating the high crystallinity of the LFP phase. LFP/Gr composite showed the existence of graphite peak at $2\theta = 26^\circ$. Hence, the graphene sheets partially stacked together by Van-der-Waals force leading to the formation of layered graphite during the formation of cathode composite. Unfortunately, the quantity of graphite in LFP/Gr was up to 5

wt.% by analyzing the XRD diagram; which might penalize the expected effect of graphene on the electrochemical performance. LFP/KB composite contains a fraction of amorphous carbon nanoparticles causing a noisy baseline and some extremely weak peaks in the XRD diagram.

According to diffraction data, the crystallite size of LFP was determined based on the Scherrer equation.

$$\tau = \frac{0.9\lambda}{\beta \times \cos \theta} \quad (1)$$

Where τ is the mean size of crystalline domains, which is smaller or equal to grain size, λ is the X-ray wavelength, β is the full width at half the maximum (FWHM) peak intensity and θ is the Bragg or diffraction angle.

In using the five strongest diffraction peaks with Miller indices: (011), (111), (121), (031) and (131), the average LFP crystallite size in the LFP/KB, LFP/CNT and LFP/Gr composites was approximately 56.4, 52.9 and 63.4 nm. These calculated values of LFP crystallite size was used only for standard comparison. Otherwise, the real examination of LFP particles size and composite morphology was performed by using TEM images.

Particle size and morphology of LFP/C composites

The morphology and microstructure of three LFP/C composites were analyzed by TEM. As shown in **Figure 2a, b, and c**, LFP particles distributed regularly in the carbon matrix. The conductive bridges were built to connect LFP particles. Hence, it could effectively enhance the electronic conductivity of LFP/C composites. Additionally, the structure of KB and CNT based LFP composite is highly porous-structure than LFP/graphene which is helpful for electrolyte penetration and facilitate the fast ion exchange or even fast discharge process. In-depth examination (**Figure 2c**), Gr sheets are folded together and supposed to form layered graphite structure as evident analyzing from XRD diagram. Consequently, the outstanding electronic conductivity of Gr was completely failed, and it's considered to be a value of graphite. Additionally, the graphite formation also diminishes the surface area of LFP preventing lithium ions moving into the bulk material under charge-discharge conditions, thus resulting in high polarization and low capacity. Through TEM images, the platelets LFP particles (**Figure 2d, e**) on the rods shape (**Figure 2f**) could be seen. Compared to the values of crystallite size from Scherrer equation (*Equation (1)*), the observed LFP grain size was larger and in range of 80-200 nm

by using the scale-bar of TEM instrument. The larger size of LFP composites was explained that the carbon coated on LFP particle to prevent the agglomeration was not entirely induced, thus, leading to a wide size distribution of LFP.

Lithium-ion diffusion kinetics

The CV measurement of three LFP/C composites was examined at various scan rates in the range of 0.01 - 0.20 mV.s⁻¹ (**Figure 3 a-c**). At each cycle, the CV profile show anodic (charge) and the cathodic (discharge) peaks corresponding to the charge - discharge reactions of the Fe³⁺/Fe²⁺ redox couple with midpoint of ~ 3.43 V during the lithium ion extraction/insertion in/out of LFP structure, which corresponds to the open-circuit voltage (OCV) of the LiFePO₄ electrode^{24,25}.

The CV profile of LFP/KB and LFP/CNT (**Figure 3 a-b**) show higher anodic and cathodic peak currents compared to that of LiFePO₄/Gr sample (**Figure 3 c**). Furthermore, the peak shapes of these composites are sharper compared to the electrode LiFePO₄/Gr, which has a broad peak indicating slower kinetics. From the CV data obtained with a scanning rate of 0.01 mV/s, the difference between the anodic and cathodic peak voltages (hysteresis) has been found to be ~0.15 V for sample LFP/CNT, whereas slightly higher values of ~0.20 V and ~0.30 V for samples LFP/KB and LFP/Gr. These results are consistent with slower kinetics and larger over-potentials exhibited by LFP/Gr.

As the scan rate increased, the charge transfer rate became faster following the significant increase of lithium ions concentration on the surface of electrode material. Thus the intensity of redox peak significantly increased.

For small scan rates, the anodic and cathodic peak currents vary linearly with the square root of the scan rate, indicating that the Li-ion insertion/extraction in LiFePO₄ is a diffuse controlled process²⁵. **Figure 3d** shows such plots for anodic currents in composites samples. According to *Randles-Sevcik* equation (*Equation (1)*), i_p versus $v^{1/2}$ is linear and the diffusion coefficient can be estimated from the slope of this line.

$$i_p = (2.69 \times 10^5) n^{3/2} v^{1/2} A D^{1/2} C^* \quad (2)$$

Where i_p is the peak current (A), n is number of electrons involved in the reaction of redox couple (for Li⁺ it is 1), v is the rate at which potential is swept (V.s⁻¹), A is the effective working electrode area (cm²), D is the diffusion coefficient of electroactive species Li⁺

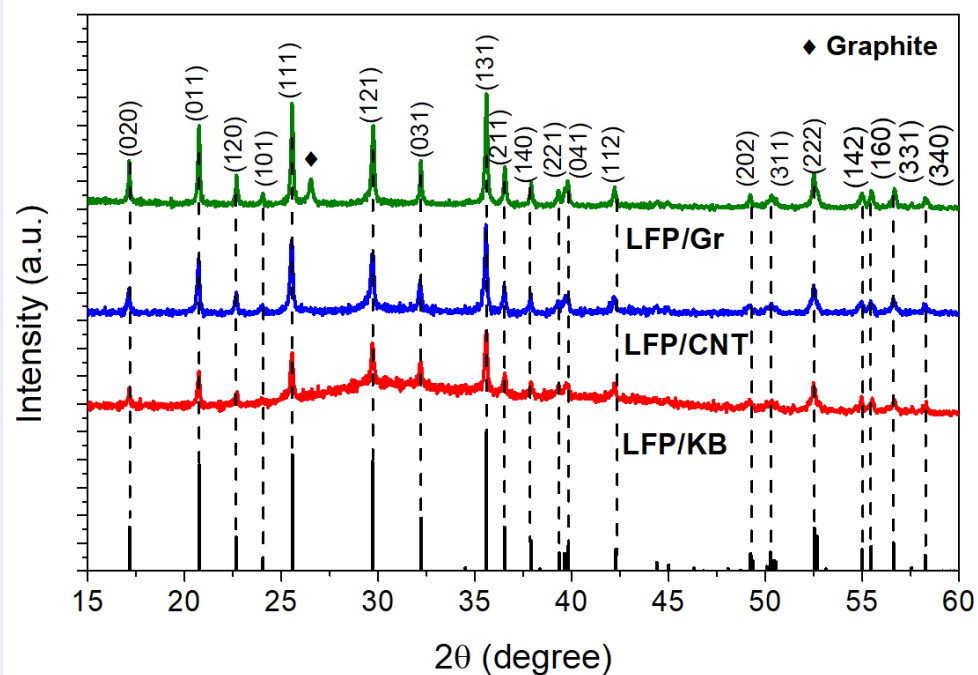


Figure 1: XRD patterns of LFP/KB, LFP/CNT and LFP/Gr composites. All diffraction patterns of three different composites are well-matched the reference patterns of LFP phase (ICDDno. 040-1499) indicated by intense peaks. Specifically, in LFP/Gr sample, a peak of graphite appeared at 26° position (ICDD no. 041-1487) illustrating their combination of graphene sheets due to Van-der-Waals force.

($\text{cm}^2 \cdot \text{s}^{-1}$) and C^* is initial concentration of Li in LiFePO_4 material (defined as the ratio bulk density to molar mass, for which the corresponding Li concentration C^* should be 0.0228 mol/cm^3).

The lithium ion diffusion coefficients of LFP/KB and LFP/CNT samples were estimated to be 3.79×10^{-11} and $2.16 \times 10^{-10} \text{ cm}^2 \cdot \text{s}^{-1}$, respectively, which is 4-6 times higher order of magnitude than that of pristine LFP (10^{-14} - $10^{-16} \text{ cm}^2 \cdot \text{s}^{-1}$) as early reported by Prosini *et al.*⁵. In contrast, lithium ion diffusion coefficient of LFP/Gr composite is $1.96 \times 10^{-16} \text{ cm}^2 \cdot \text{s}^{-1}$, which is quite like the original LFP.

DISCUSSION

As expected, coating LFP particles with conductive carbon are the predominant way to enhance electrical conduction within an insulating LFP cathode. In the solvothermal process, the nanosized particles could be effectively controlled by the solvothermal method in modifying different parameters (pH, chemical agents...). While using the carbon matrix, the LFP particles were physically dispersed into carbon matrix and well-connected with carbon particles or carbon tubes, as obviously seen in case of LFP/KB

or LFP/CNT (Figure 2 d-e). Nevertheless, the synthesis pathway isn't effective to disperse LFP carbon into the graphene sheets due to high Van-der-Waals force between graphene layers even with the vigorous stirring. As a result, the graphene layers were stacked together and destroyed the superior electronic conductor (Figure 2 f).

Cyclic Voltammetry (CV) is a common technique for studying the properties of an electrochemical system. Within the scanning potential range, a current peak occurs at a certain potential indicating an occurrence of an electrode reaction. In the case of LiFePO_4 electrode, the two peaks are expectedly observed around 3.45 V vs. Li^+/Li , correspond to the two-phase charge-discharge reaction of $\text{Fe}^{3+}/\text{Fe}^{2+}$ redox couple. By analyzing the resultant current versus potential profiles, information on the kinetics and thermodynamics of the electrode reaction can be obtained²⁴. CV measurements confirmed the significant enhancement of electrochemical kinetic of LFP/KB and LFP/CNT composite electrodes through the calculation of lithium ion diffusion. Due to expected role of tailored carbon materials (carbon KB, carbon nanotubes), during the reduction reaction,

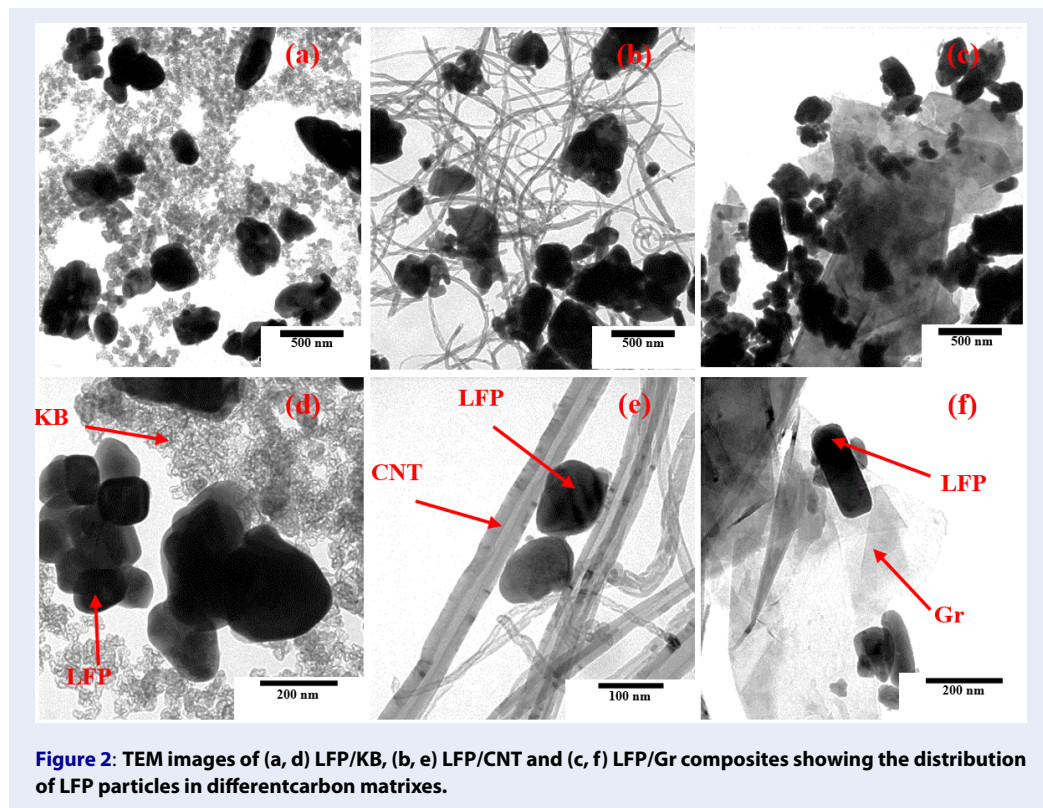


Figure 2: TEM images of (a, d) LFP/KB, (b, e) LFP/CNT and (c, f) LFP/Gr composites showing the distribution of LFP particles in different carbon matrixes.

electrons transfer rapidly into Fe d-orbitals of LFP compound and simultaneously formed electrostatic forces attracting lithium ions to diffuse along the electrode surface and then go into host matrix for charge neutralization. The composite LFP/Gr didn't get any benefit from the superior electronic conductivity of graphene due to stacked layers; indeed, the electrochemical performance was nearly penalized. Therefore, pre-treatment or modification of graphene surface should be considered to eliminate restacking phenomenon of Gr sheets before mixing them into desired composites.

CONCLUSIONS

LFP/KB, LFP/CNT and LFP/Gr composites were successfully obtained by physical mixing assisted solvothermal process. LFP particles distributed regularly in carbon matrix with the grain size ranging from 80-200 nm. Regarding the electrochemical performance, the synthesized LFP composites showed excellent ion diffusion coefficient compared to pristine LFP, except for LFP/Gr. Additionally, based on the calculated values, KB and CNT based LFP composite almost had a good impact on the electrochemical kinetics of lithium diffusion. Concerning the commercialization, KB could be a potential candidate

for large-scale production due to low-cost, stable and high electrochemical performance.

ABBREVIATIONS

CNT: Carbon nanotubes
 CV : Cyclic Voltammetry
 Gr : Graphene
 KB: Carbon Ketjen
 LFP: LiFePO₄

COMPETING INTERESTS

The authors declare that there is no conflict of interest regarding the publication of this article

AUTHORS' CONTRIBUTIONS

All the authors contribute equally to the paper including the research idea, experimental section and written manuscript.

ACKNOWLEDGMENTS

This work is funded by Viet Nam National University of Ho Chi Minh city (VNU HCM) through research grant NV2018-18-01 and Department of Science and Technology of Ho Chi Minh city through project grant number 107/2016/HD-SKHCN.

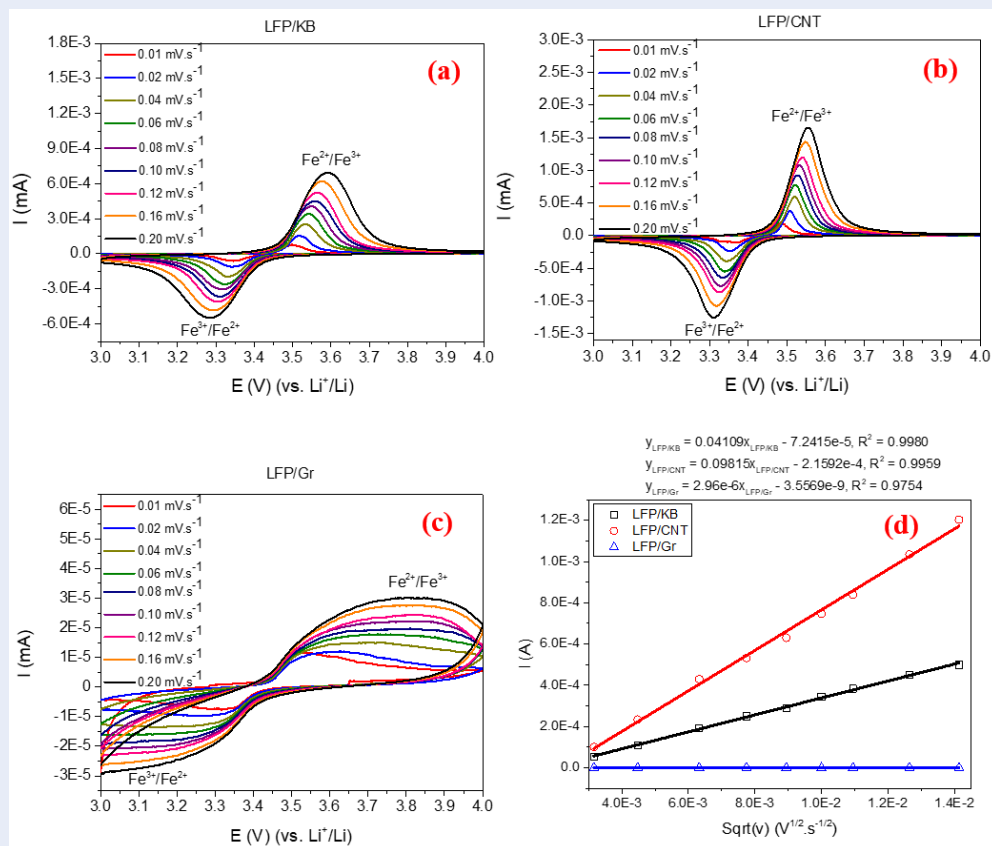


Figure 3: Cyclic voltammograms of (a) LFP/KB, (b) LFP/CNT and (c) LFP/Gr composite electrodes at different scan rates. The oxidation state of LFP within two-phase transition is indicated by pair of peaks around 3.45 V (vs. Li⁺/Li). **(d)** Linear correlation between *i_p* and square root of scan rates for LFP/KB, LFP/CNT and LFP/Gr samples.

REFERENCES

- Bruce PG, Scrosati B, Tarascon JM. Nanomaterials for rechargeable lithium batteries. *Angew Chem Int Ed Engl.* 2008;47(16):2930–46. 18338357. Available from: [10.1002/anie.200702505](https://doi.org/10.1002/anie.200702505).
- Goodenough JB, Kim Y. Challenges for Rechargeable Li Batteries. *Chem Mater.* 2010;22(3):587–603. Available from: [10.1021/cm901452z](https://doi.org/10.1021/cm901452z).
- Wagemaker M, Mulder FM. Properties and promises of nano-sized insertion materials for Li-ion batteries. *Acc Chem Res.* 2013;46(5):1206–15. 22324286. Available from: [10.1021/ar2001793](https://doi.org/10.1021/ar2001793).
- Padhi AK, Nanjundaswamy KS, Goodenough JB. Phospho-olivines as positive-electrode materials for rechargeable lithium batteries. *J Electrochem Soc.* 1997;144(4):1188–94. Available from: [10.1149/1.1837571](https://doi.org/10.1149/1.1837571).
- Prosini PP, Lisi M, Zane D, Pasquali M. Determination of the chemical diffusion coefficient of lithium in LiFePO₄. *Solid State Ion.* 2002;148(1-2):45–51. Available from: [10.1016/S0167-2738\(02\)00134-0](https://doi.org/10.1016/S0167-2738(02)00134-0).
- Amin R, Balaya P, Maier J. Anisotropy of electronic and ionic transport in LiFePO₄ single crystals. *Electrochem Solid-State Lett.* 2007;10(1):13–6. Available from: [10.1149/1.2388240](https://doi.org/10.1149/1.2388240).
- Wang J, Sun X. Understanding and recent development of carbon coating on LiFePO₄ cathode materials for lithium-ion batteries. *Energy Environ Sci.* 2012;5(1):5163–85. Available from: [10.1039/C1EE01263K](https://doi.org/10.1039/C1EE01263K).
- Yuan LX, Wang ZH, Zhang WX, Hu XL, Chen JT, Huang YH, et al. Development and challenges of LiFePO₄ cathode material for lithium-ion batteries. *Energy Environ Sci.* 2011;4(2):269–84. Available from: [10.1039/C0EE00029A](https://doi.org/10.1039/C0EE00029A).
- Kang B, Ceder G. Battery materials for ultrafast charging and discharging. *Nature.* 2009;458(7235):190–3. 19279634. Available from: [10.1038/nature07853](https://doi.org/10.1038/nature07853).
- Ni H, Liu J, Fan LZ. Carbon-coated LiFePO₄-porous carbon composites as cathode materials for lithium ion batteries. *Nanoscale.* 2013;5(5):2164–8. 23389625. Available from: [10.1039/c2nr33183g](https://doi.org/10.1039/c2nr33183g).
- Cheng F, Wang S, Lu AH, Li WC. Immobilization of Nanosized LiFePO₄ Spheres by 3D Coraloid Carbon Structure with Large Pore Volume and Thin Walls for High Power Lithium-Ion Batteries. *J Power Sources.* 2013;229:249–57. Available from: [10.1016/j.jpowsour.2012.12.036](https://doi.org/10.1016/j.jpowsour.2012.12.036).
- Younesi R, Christiansen AS, Scipioni R, Ngo DT, Simonsen SB, Edstrom K, et al. Analysis of the interphase on carbon black formed in high voltage batteries. *J Electrochem Soc.* 2015;162(7):1289–96. Available from: [10.1149/2.0761507jes](https://doi.org/10.1149/2.0761507jes).
- Xie HM, Wang RS, Ying JR, Zhang LY, Jalbout AF, Yu HY, et al. Optimized LiFePO₄-polyacene cathode material for lithium-ion batteries. *Adv Mater.* 2006;18(19):2609–13. Available from: [10.1002/adma.200600578](https://doi.org/10.1002/adma.200600578).
- Yang X, Xu Y, Zhang H, Huang Y, Jiang Q, Zhao C. Enhanced high rate and low-temperature performances of mesoporous LiFePO₄/Ketjen Black nanocomposite cathode material. *Electrochim Acta.* 2013;114:259–64. Available from: [10.1016/j](https://doi.org/10.1016/j)

- electacta.2013.10.037.
15. Shu J, Shui M, Huang F, Xu D, Ren Y, Hou L, et al. Surface behaviors of conductive acetylene black for lithium-ion batteries at extreme working temperatures. *J Phys Chem C*. 2011;115(14):6954–60. Available from: [10.1021/jp200167x](https://doi.org/10.1021/jp200167x).
 16. Prasek J, Drbohlavova J, Chomoucka J, Hubalek J, Jasek O, Adam V, et al. Methods for carbon nanotubes synthesis. *J Mater Chem*. 2011;21(40):15872–84. Available from: [10.1039/c1jm12254a](https://doi.org/10.1039/c1jm12254a).
 17. Yang J, Wang J, Tang Y, Wang D, Xiao B, Li X, et al. In situ self-catalyzed formation of core-shell LiFePO₄@CNT nanowires for high rate performance lithium-ion batteries. *J Mater Chem A Mater Energy Sustain*. 2013;1(25):7306–11. Available from: [10.1039/c3ta11262d](https://doi.org/10.1039/c3ta11262d).
 18. Wu XL, Guo YG, Su J, Xiong JW, Zhang YL, Wan LJ. Carbon-nanotube-decorated nano-LiFePO₄@C cathode material with superior high-rate and low-temperature performances for lithium-ion batteries. *Adv Energy Mater*. 2013;3(9):1155–60. Available from: [10.1002/aenm.201300159](https://doi.org/10.1002/aenm.201300159).
 19. Thorat IV, Mathur V, Harb JN, Wheeler DR. Performance of carbon-fiber-containing LiFePO₄ cathodes for high-power applications. *J Power Sources*. 2006;162(1):673–8. Available from: [10.1016/j.jpowsour.2006.06.032](https://doi.org/10.1016/j.jpowsour.2006.06.032).
 20. Wu CY, Cao GS, Yu HM, Xie J, Zhao XB. In situ synthesis of LiFePO₄/carbon fiber composite by chemical vapor deposition with improved electrochemical performance. *J Phys Chem C*. 2011;115(46):23090–5. Available from: [10.1021/jp205146d](https://doi.org/10.1021/jp205146d).
 21. Botas C, Alvarez P, Blanco P, Granda M, Blanco C, Santamaria R, et al. Graphene materials with different structures prepared from the same graphite by the Hummers and Brodie methods. *Carbon*. 2013;65:156–64. Available from: [10.1016/j.carbon.2013.08.009](https://doi.org/10.1016/j.carbon.2013.08.009).
 22. Zhang Y, Wang W, Li P, Fu Y, Ma X. A simple solvothermal route to synthesize graphene-modified LiFePO₄ cathode for high power lithium ion batteries. *J Power Sources*. 2012;210:47–53. Available from: [10.1016/j.jpowsour.2012.03.007](https://doi.org/10.1016/j.jpowsour.2012.03.007).
 23. Nakamura T, Miwa Y, Tabuchi M, Yamada Y. Structural and surface modifications of LiFePO₄ olivine particles and their electrochemical properties. *Journal of The Electrochemical Society*. 2006;p. A1108–A1114.
 24. Bard AJ, Faulkner LR. *Electrochemical Methods Fundamental and Applications*. New York: Jon Wiley & Sons; 1980. .
 25. Yu DY, Fietzek C, Weydanz W, Donoue K, Inoue T, Kurokawa H, et al. Study of LiFePO₄ by Cyclic Voltammetry. *J Electrochem Soc*. 2007;154(4):253–7. Available from: [10.1149/1.2434687](https://doi.org/10.1149/1.2434687).

